CHARACTERIZING THE MINIMUM IGNITION ENERGY OF COMMON REFRIGERANTS IN A 20 L VESSEL

Jessica C. DEMOTT*, Damien RODOWSKI*, Chad MASHUGA**

*Arkema Inc., King of Prussia, PA, 19406, U.S.A.

**Department of Chemical Engineering, Texas A&M University, College Station, TX, 77843, U.S.A.

ABSTRACT

Minimum ignition energy (MIE) can be defined as the minimum electrical energy discharged from a capacitor, which is just sufficient to effect ignition of the most easily ignitable concentration of the fuel in air. Although MIE's are essential information for the safe handling of fuels such as refrigerants, reported literature values vary widely and often consist of a single reported value rather than a curve showing a minima. The need for an improved understanding of MIE is made apparent by the continuing occurrence of incidents in the process industries. This publication addresses some gaps in the reported literature with respect to this topic. In this study, the minimum ignition characteristics of six refrigerants were determined. In particular, two of the refrigerants were examined at 50% relative humidity using a novel testing approach. Each of the MIE's were found using a 20 L vessel resulting in energy-concentration curves demonstrating a minima. Experimental values are compared to reported literature values. The MIE's were consistent with the single point values reported in literature, while the two humidified refrigerants were not as consistent. To that end, this work offers additional considerations relative to some of the reported values and provides suggestions for improvements in the testing apparatus.

Keywords: Refrigerants; Minimum Ignition Energy; Combustion; Flammability

INTRODUCTION

The minimum ignition energy (MIE) can be defined as the lowest spark energy required that is just sufficient to ignite the most ignitable fuel-air mixture. The most ignitable fuel-air mixture, including the most ignitable refrigerant-air mixture, is a composition between the lower and upper flammable limit (LFL and UFL), and near but just richer than the stoichiometric mixture as shown in Fig. 1.

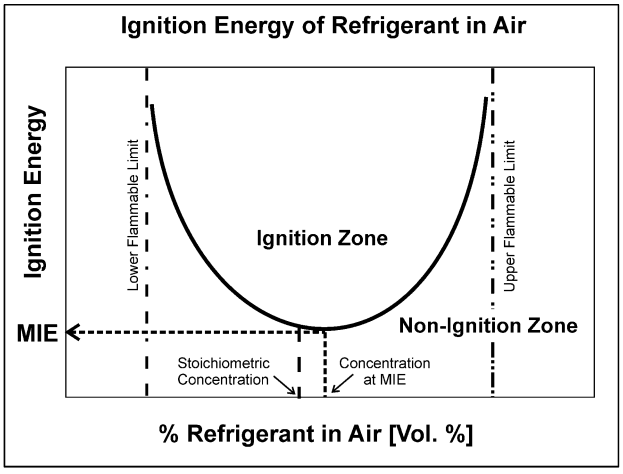

Fig. 1 Typical ignition energy and refrigerant-air concentration curve showing the ignition and non-ignition zone.

The designation of the ignition zone and the non-ignition zone in Fig. 1 is determined by conducting experiments at various energies and compositions as shown in Fig. 2.

In Fig. 2 for a given energy level and refrigerant-air concentration, the mixture either ignites (square) or results in no ignition (circle). These ignitions and non-ignitions define the ignition and non-ignition boundary, allowing MIE determination.

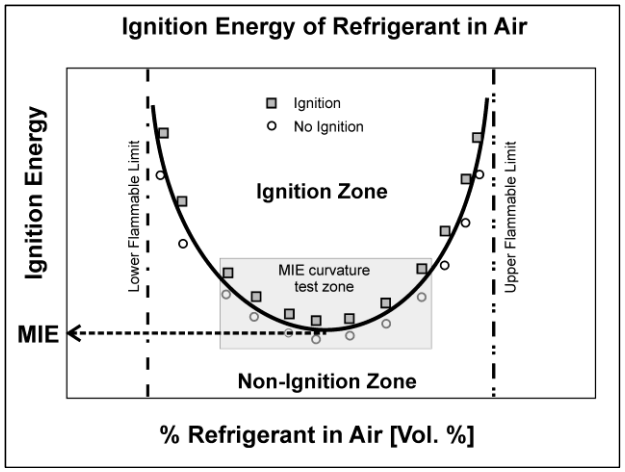

Fig. 2 Idealized experimental determination of the ignition and non-ignition zones, permitting MIE determination.

The understanding of the ignition and non-ignition zones, as well as the MIE value shown in Fig. 2 provides critical understanding for the hazard assessment of refrigerant manufacture, transport, storage, and use. The MIE is a relative indicator of the probability of a refrigerant ignition if released. Thus, the MIE is an important single value that permits a relative comparison of the safety and

hazard assessment of various refrigerates.

OBJECTIVES OF THIS WORK

For safe handling of fuels, including refrigerants, an understanding of its MIE is essential. However, the literature often reports single, widely varying values[1], instead of a data set showing curvature with a defined MIE value. Additionally, literature data is often from several researchers, where various equipment and techniques were deployed, perhaps contributing variation in the reported literature.

The main objective of this work is to produce high quality refrigerant MIE data for six common refrigerants. This data will include a sufficient quantity and quality to permit resolution of the MIE through curvature in the ignition energy vs. refrigerant-air concentration graph as shown in Fig. 2, highlighted by the gray MIE curvature test zone.

To accomplish this main objective, careful gas blending must be performed with the refrigerant and air. Next a sufficient volume of this mixture must be ignited in order to represent the real-world credible scenario and to avoid overdriving the combustion process for the often difficult to ignite halocarbon refrigerants[2]. Finally, a highly repeatable ignition system is needed with a wide range of energies to match the inherent range in old and new refrigerants.

In summary the objectives of this work are:

[1] Develop an accurate and repeatable gas blending System.
[2] Establish a large test volume system suitable for Refrigerants.
[3] Develop a wideband spark ignition device with high Repeatability.
[4] Measure 6 MIE curves for common refrigerants.

EXPERIMENTAL APPARATUS AND METHODS

To satisfy the first objective of developing an accurate and repeatable gas blending system, the author improved upon a system first developed for his PhD dissertation[3-5] shown in Figs. 3 and 4. The gas blending system is highly automated with a custom LabVIEW program for both control of the gas blending and data acquisition for the deflagration testing.

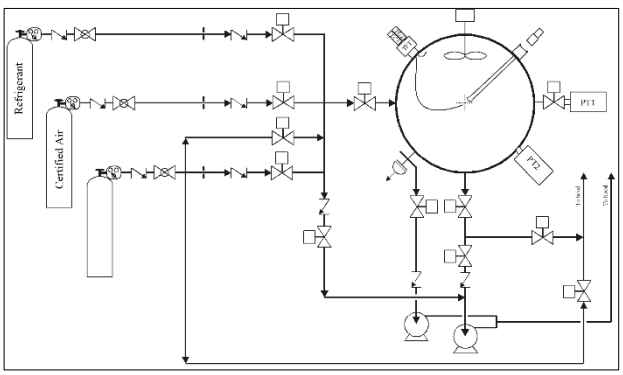

Fig. 3 Piping and instrument diagram for the automated 20 L multi gas flammability apparatus.

The apparatus utilizes fast acting solenoid valves and a pressure transducer (0.05% accuracy) to control the gas blending. The gas blending transducer has a 0 – 25 psia range and is isolated from the combustion pressure by a valve. The combustion pressure is tracked by a transducer (0.1% accuracy) that is mounted with its membrane on the vessel wall.

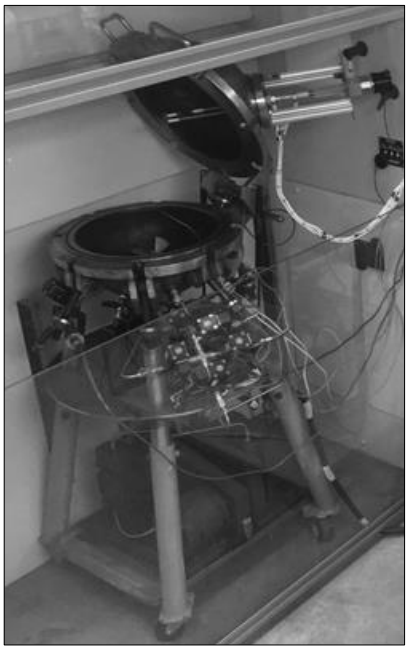

Fig. 4 Automated 20 L multi gas flammability apparatus.

To satisfy the second objective of this work, to establish a large volume test system suitable for refrigerants, a 20 L vessel is selected. It is sufficiently large for refrigerant flammability and minimum ignition energy testing and better matches actual credible scenarios due to its scale. The vessel is constructed of 304 stainless steel and has an internal volume of 20 L. Inside the vessel there is a mixing propeller that is magnetically coupled with a drive motor mounted externally to the vessel to ensure fast and complete equilibrium when gas blending. Shown in Fig. 4, the system uses two vacuum pumps, one is chemical duty vacuum pump, while the other is a standard oil-sealed rotary vane pump. After refrigerant ignition, the gaseous HF is removed from the vessel with the chemical duty pump and delivered to an amine scrubber system. The gas exiting the amine scrubber is monitored for HF with a sensor capable of +/- 0.1 ppm HF. Once three pressure-vacuum purge cycles pass through the amine absorber, the standard oil pump is used to pressure-vacuum purge the vessel for the next test.

Gas blending advancements for this work involve the establishment of a thermodynamic criteria necessary to achieve an equilibrium during the partial pressure gas loading process. During the initial pressure determination or the determination of the partial pressures, a thermal and baric criteria is applied. This includes examining the departures of dT, dT/dt, dP, and dP/dt from setpoints for the system.

Where;
dT is the departure from the gas test temperature setpoint,
dT/dt is the rate of temperature change after gas loading,
dP is the departure from the gas test pressure setpoint,
dP/dt is the rate of pressure change after gas loading.
During gas blending if any one of these parameters is outside the setpoint, the system is considered to not be at equilibrium. After further mixing and the above conditions satisfied, the pressure is measured and gas blending continues, or ignition testing can proceed.
In order to satisfy the third objective of developing a wideband spark ignition device, it is necessary to examine the typical ways in which a spark ignition system can be designed. The use of a capacitive spark for MIE testing replicates the real-world credible scenario of an electrostatic discharge as an ignition source. Capacitive sparks for MIE testing are primarily produced by two circuit approaches shown in Fig. 5 and Fig. 6. Both approaches have several advantages and disadvantages and will be discussed further.

Fig. 5 shows a typical fixed spark gap ignition system, often used for producing very low energy capacitive sparks[6].

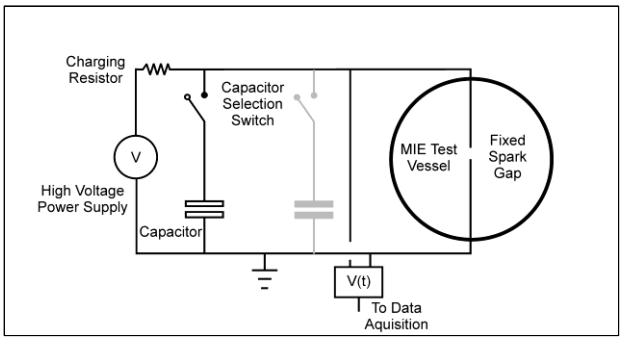

Fig. 5 Fixed gap spark ignition generation circuit.

In Fig. 5 the fixed spark gap ignition generation circuit is operated by the following steps:
[1] Based on desired energy, capacitor(s) are switched on (often manually).
[2] The high voltage power supply slowly charges the capacitor(s) (often via $\tau = RC$).
[3] When the capacitor voltage exceeds the breakdown voltage of the gas mixture, a spark discharge results.
[4] The spark energy is determined by Eq. 1 below:

$$E = \frac{1}{2}C\left(V_i^2 - V_f^2\right) \quad (1)$$

where;
E is the resulting spark energy (Joules),
C is the value of the capacitor(s) (Farads),
V_i is the initial voltage on the capacitor just before spark formation (volts),
V_f is the residual voltage on the capacitor(s) after spark formation (volts).
There are several important disadvantages of this approach. First, the input impedance of the voltage measurement before (V_i) and after (V_f) the spark formation can change the voltage value being measured, resulting in inaccuracy. Depending on the system design, the capacitor may recharge after initial discharge, resulting in multiple sparks and an unknown energy delivery. Finally, a fixed spark gap requires knowing both the voltage and capacitance needed to produce a desired spark energy. This greatly complicates testing in mapping the ignition and non-ignition zones with the ignition and no ignition points as shown in Fig. 2.
Fig. 6 shows a second approach and circuit for producing capacitive sparks for MIE testing.

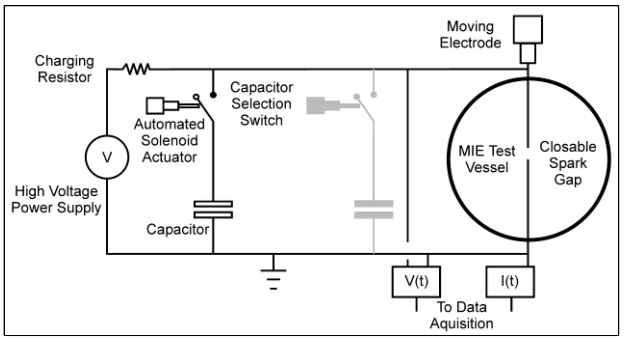

Fig. 6 Moving electrode spark ignition generation circuit.

This general approach was used to satisfy the third objective of developing a wideband spark ignition device for this work. The device, shown in Fig. 7, has an ability to deliver ignition energies from 0.004 mJ – 130 J, thus it is referred to as a wideband ignition device. Both control and data acquisition with the device has been highly automated using LabVIEW to eliminate inaccuracy and improve MIE testing efficiency.

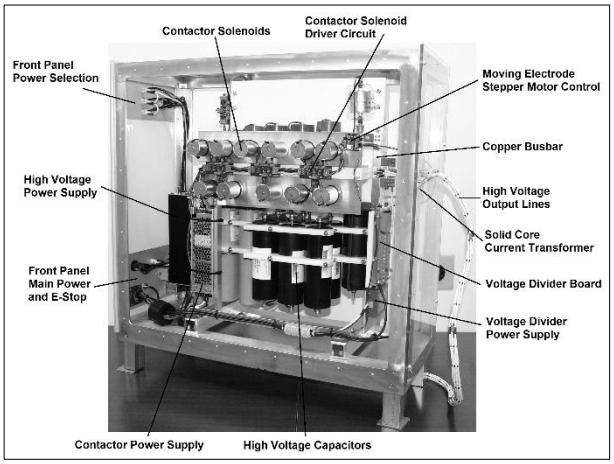

Fig. 7 Components of the Wideband spark ignition apparatus.

The wideband ignition device is operated by the following steps:
[1] The desired ignition energy (E) is entered into the LabVIEW program.
[2] Based on E, capacitor(s) are automatically switched onto the high voltage (HV) busbar.

[3] Based on *E*, the HV power supply automatically charges the capacitor(s) to the V_i.
[4] The HV power supply is automatically disconnected from the busbar.
[5] The tungsten electrode gap is automatically closed while monitoring the dynamic busbar voltage (*V(t)*) and the delivered current (*I(t)*) to the spark gap.
[6] During gap closure, spark over occurs and the capacitor(s) voltage is measured μsec before discharge (V_i), along with the spark gap distance.
[7] After spark formation the electrode is retracted to the home position and the residual voltage on the capacitor(s) is measured (V_f).
The delivered energy in the spark discharge is determined by Eq. 1 presented previously. Additionally, a second independent method is also used shown in Eq. 2.

$$E = \int_0^t V(t)I(t)dt = \int_0^t P(t)dt \qquad (2)$$

Where;
E is the resulting spark energy (Joules),
V(t) is the dynamic voltage during the spark discharge,
I(t) is the dynamic current during the spark discharge,
P(t) is the dynamic power delivered during the spark discharge.
Fig. 8 shows an example of the *V(t)* and *I(t)* collected by the automated wideband ignition device for a 25 mJ spark. By Eq. 1 the resulting spark energy is found to be 25.84 mJ, while Eq. 2 finds 25.64 mJ.

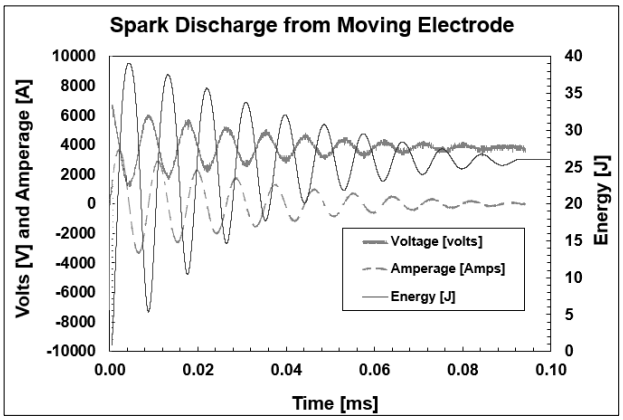

Fig. 8 Wideband spark device data capture for voltage and current during a *E* = 25 mJ spark.

RESULTS AND DISCUSSION

To accomplish the fourth objective of this work, the automated 20 L apparatus and the wideband spark device were used to measure the MIE curves for six refrigerants (R152a, R32, R457A, R457B, R1234yf and R1234ze). R1234yf and R1234ze were evaluated with air containing 50% relative humidity, all others with dry air. The air used in this work was blended from cryogenic sources and by analysis was found to be 20.7% oxygen, 79.3% nitrogen and 0.250 ppm moisture. In the 20 L vessel, the criteria for flammability was any post ignition pressure rise greater than the pressure contribution of the spark ignition. All tests were conducted at 23 °C and an initial pressure of 14.67 psia.
Fig. 9 shows the MIE curve for R152a (1,1-difluoroethane) in dry air. The R152a MIE was found to be 1.00 < MIE < 1.97 mJ, with an estimated value of E_s = 1.49 mJ. There is good agreement with the only MIE curve that could be found in literature[7]. This is evidence that the gas blending of the 20 L apparatus and the delivered spark energy of the wideband ignition device are very consistent.
Fig. 10 shows the MIE curve for R32 (difluoromethane) in dry air. The R32 MIE was found to be 82 < MIE < 86 mJ, with an estimated value of E_s = 84 mJ. No MIE curves were found in literature, however a range of 30 < MIE < 100 mJ is often reported[8], which compares well with the results of this work. Numerous non-sequential tests were performed for R32 to resolve the repeatability of the MIE test results. The test order and data series (% R32 in air) are listed in Table 1. Fig. 10 also shows the test series number above the data.

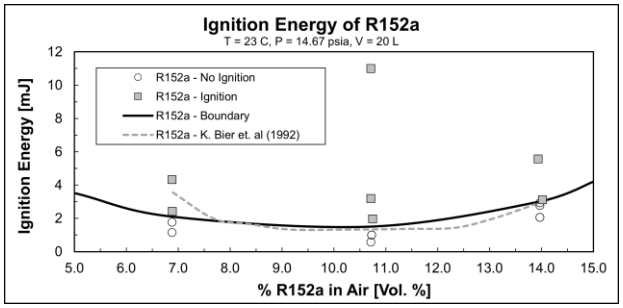

Fig. 9 Minimum ignition energy curve for R152a in dry air.

From Fig. 10 series pairs (1-2, 3-4, 5-6) are all indicating the same boundary between ignition and no ignition. Series 7, 8 and 9 provide further resolution of the boundary between ignition and no ignition. This is evidence that the gas blending of the 20 L apparatus and the delivered energy of the wideband ignition device are very consistent and compare well with reported ranges of MIE in literature.

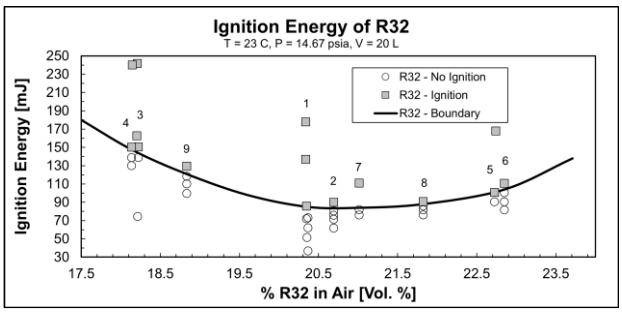

Fig. 10 Minimum ignition energy curve for R32 in dry air.

Table 1 Data serries sequence for R32

Test Order	Data Series [% R32 in Air]
1	20.34
2	20.69
3	18.22
4	18.14
5	22.72
6	22.85
7	21.01
8	21.82
9	18.83

Fig. 11 shows the MIE curve for R457A (70% 2,3,3,3-tetrafluoropropene, 18% difluoromethane, 12% 1,1-difluoroethane) in dry air. The R457A MIE was found to be 78 < MIE < 90 mJ, with an estimated value of E_s = 84 mJ. There is good agreement with the MIE curve found by a third party testing laboratory which found 50 < MIE < 70 mJ, with an estimated value of E_s = 60 mJ. No literature values or curves were found for R457A. This is further evidence of the accuracy and repeatability of the 20 L apparatus and the wideband ignition device.

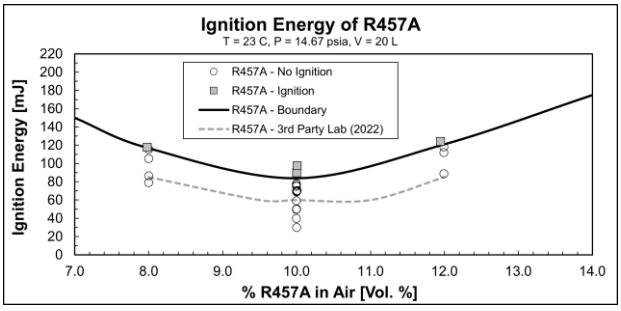

Fig. 11 Minimum ignition energy curve for R475A in dry air.

Fig. 12 shows the MIE curve for R457B (55% 2,3,3,3-tetrafluoropropene, 35% difluoromethane, 10% 1,1-difluoroethane) in dry air. The R457B MIE was found to be 99 < MIE < 108 mJ, with an estimated value of E_s = 103.5 mJ. No literature MIE curves, MIE ranges or single MIE values could be found.

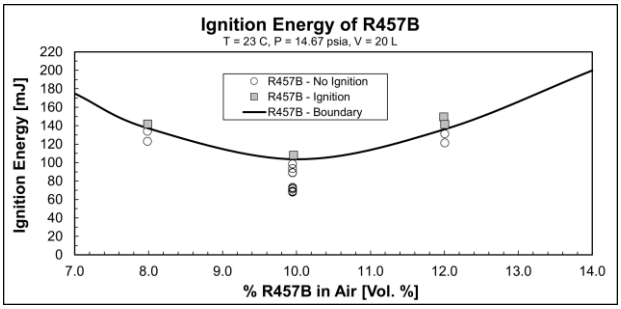

Fig. 12 Minimum energy curve for R475B in dry air.

The compositions of R457A and R457B are shown in Table 2. The MIE values of the constituents that make up R457A and R457B, and the MIE values of the R457A and R457B mixtures from this work are also shown in Table 2.

Eq. 3 shows a molar weighted MIE contribution equation which can permit a relative comparison of mixture MIE values but does not estimate or predict the actual MIE value.

$$E_s = \sum_i^N y_i MIE_i \quad (3)$$

If Eq. 3 is used with the compositional data for R457A and R457B and the results of this work, it predicts the MIE of R457A would be greater than that of R457B. However, if the contribution of R1234yf is ignored, Eq. 3 predicts the MIE of R457B is greater than that of R457A which agrees with the results of this work. Ignoring the contribution of R1234yf may be justified since its MIE value is much further away from the relatively close values of R32 and R152a.

Table 2 R457A and R457B compositions and the MIEs found in this work.

	MIE (this work) [mJ]	R457A [vol.%]	R457B [vol.%]
R1234yf	1962	70	55
R32	84	18	35
R152a	1.49	12	10
$E_s = \Sigma y_i MIE_i$	Predicts $MIE_{R457A} > MIE_{R457B}$		
R1234yf	Not used	0	0
R32	84	60	78
R152a	1.49	40	22
$E_s = \Sigma y_i MIE_i$	Predicts $MIE_{R457B} > MIE_{R457A}$		
MIE (this work)		84	103.5

Fig 13 shows the MIE curve for R1234yf (2,3,3,3-tetrafluoropropene) in air containing 50% relative humidity. A liquid injection technique and system was developed to achieve the 50% relative humidity for this work. The R1234yf MIE was found to be 1850 < MIE < 2075 mJ, with an estimated value of E_s = 1962 mJ. With humidity, literature typically reports the R1234yf MIE to be 5,000 < MIE < 10,000 mJ [9]. No MIE curves were found in literature supporting this humid MIE range. A single MIE curve was found in literature[10] and is presented in Fig. 13.

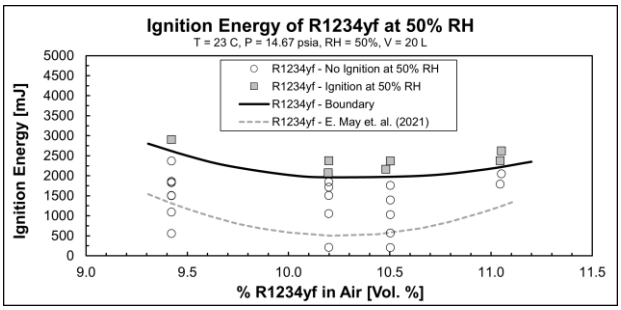

Fig.13 Minimum ignition energy curve for R1234yf (2,3,3,3-tetrafluoropropene) in air with 50% relative humidity.

Fig. 14 shows the MIE curve for R1234ze (trans-1,3,3,3-tetrafluoroprop-1-ene) in air containing 50% relative humidity. The R1234ze MIE was found to be 3578 < MIE < 3865 mJ, with an estimated value of E_s = 3721 mJ. Literature reports no ignition for dry R1234ze at 20 °C, and an MIE of 61,000 < MIE < 64,000 mJ at 54 °C[11].

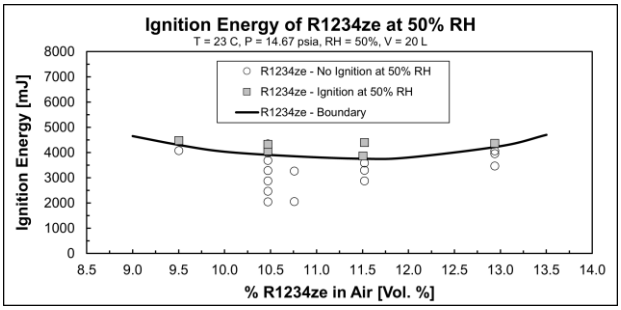

Fig. 14 Minimum ignition energy curve for R1234ze in air with 50% relative humidity.

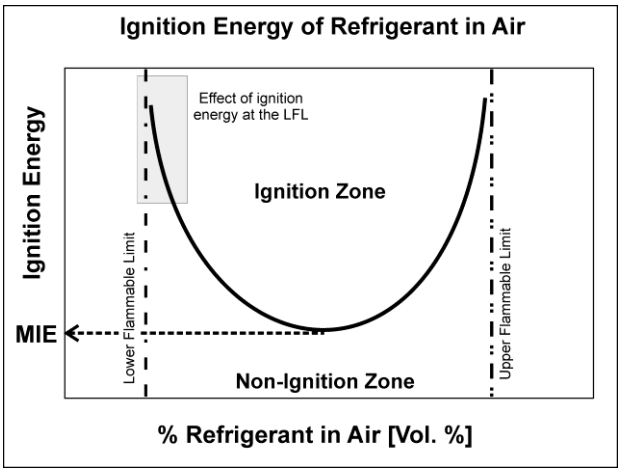

Fig. 15 Traditional MIE and the effect of ignition energy around the lower flammable limit.

The MIE measures the lowest ignition energy near the stochiometric concentration of the refrigerant in air. During a refrigerant leak, achieving a near stoichiometric mixture is a lower probability scenario. A more credible scenario is the gradual, semi-confined accumulation of refrigerant in air, approaching the LFL. Thus, a more credible hazard assessment associated with a refrigerant would be the effect of ignition energy around the LFL as shown in the gray box in Fig. 15. The wideband spark device was adapted to the ASTM E681 12 L test device[12] to develop the ignition energy vs. concentration curve near the LFL. Fig. 16 shows the effect of ignition energy near the LFL for R152a in dry air using the ASTM E681 12 L test method. Data of this type could be used to examine the likelihood of a range of concentrations and potential ignition energies being present for scenario hazard assessment. It provides a more realistic use than the traditional MIE values at stochiometric refrigerant in air.

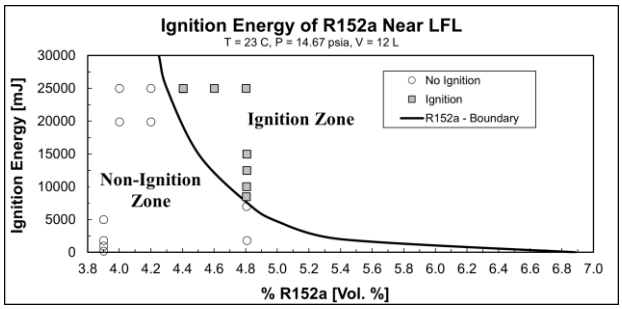

Fig. 16 The effect of ignition energy near the LFL for R152a in dry air using the ASTM E681 12 L test method.

CONCLUSIONS

The goals of this work were to:

[1] Develop an accurate and repeatable gas blending System.
[2] Establish a large volume test system suitable for Refrigerants.
[3] Develop a wideband spark ignition device with high Repeatability.
[4] Measure 6 MIE curves for common refrigerants.

With the advancement of the 20 L apparatus and development of the wideband spark device, goals 1-3 are accomplished. Sufficient ignition energy measurements were made resulting in MIE curves for six refrigerants (R152a, R32, R457A, R457B, R1234yf and R1234ze). The MIE curves for R1234yf and R1234ze used certified air containing 50% relative humidity while all others used dry certified air. Good agreement was found with available literature data, which is evidence that the gas blending of the 20 L apparatus and the delivered energy of the wideband ignition device are very consistent and accurate.

The wideband ignition device was adapted to the ASTM E681 12 L test system, permitting the development of an ignition curve near the LFL. A more credible hazard assessment results from the understanding of the more credible scenario of a refrigerant leak approaching the LFL. In several ways this data is more useful and relevant for hazard assessment than traditional MIE measurements.

NOMENCLATURE

MIE	: minimum ignition energy, mJ
LFL	: lower flammable limit in air, vol. %
UFL	: upper flammable limit in air, vol. %
dT	: departure from the gas test temperature setpoint, °C
dT/dt	: rate of temperature change after gas loading, °C/min
dP	: departure from the test pressure setpoint, psia
dP/dt	: rate of pressure change after gas loading, psia/min
E	: resulting spark energy, J
C	: capacitor value, F
R	: resistance in the spark circuit, Ω
τ	: time constant capacitor-resistance circuit, s
V_i	: initial capacitor voltage just before spark, V
V_f	: final capacitor voltage just after spark, V
$V(t)$	: dynamic voltage during the spark, V
$I(t)$	: dynamic current during the spark, A
$P(t)$	: dynamic power during the spark, W
E_s	: estimated MIE between go & no-go, J
y_i	: mole fraction of i^{th} material
$MIEi$	: MIE of i^{th} material in a mixture, J

REFERENCES

[1] V. Babrauskas, “Minimum Values of Voltage, Current, or Power for the Ignition of Fire.” *Fire*, 5(6), 201(2022).

[2] R. Richard, “Flammability testing in large volume vessels” The Air-conditioning and Refrigeration Technology Institute, Project 655-52400, 1998.

[3] C. Mashuga, D. Crowl, “Application of the Flammability Diagram for Evaluation of Fire and Explosion Hazards of Flammable Vapors.” *Process Safety Progress*, 17(3) 1998.

[4] C. Mashuga, “Determination of the Combustion Behavior for Pure Components and Mixtures Using a 20-Liter Sphere.” 1999.

[5] C. Mashuga, D. Crowl “Problems with Identifying a Standard Procedure for Determining KG Values for Flammable Vapors.” *Journal of Loss Prevention in the Process Industries*, 13(3-5), 369(2000).

[6] Bane, S.P.M., et al. “Statistical Analysis of Electrostatic Spark Ignition of Lean H2/O2/Ar Mixtures.” *International Journal of Hydrogen Energy*, 36(3), 2344(2022).

[7] W. Leuckel, B. Leisenheimer, K Bier, Combustion properties of the refrigerant R512a and its mixture with R134a or R23, 113(1992).

[8] B. Minor, Barbara, M. Spatz. *HFO-1234yf Low GWP Refrigerant Update*, International Refrigeration and Air Conditioning Conference, 937 (2008).

[9] B. Minor et al. “Flammability Characteristics of HFO-1234yf.” *Process Safety Progress*, 29(2), 150(2009).

[10] M. Sadaghiani et al. “Minimum Ignition Energies and Laminar Burning Velocities of Ammonia, HFO-1234yf, HFC-32 and Their Mixtures with Carbon Dioxide, HFC-125 and HFC-134a.” *Journal of Hazardous Materials*, 407, 124781(2021).

[11] Honeywell Brochure, Fourth Generation Refrigerants for the 21st Century, 2025.

[12] ASTM E681-09(2025). Standard Test Method for Concentration Limits of Flammability of Chemicals (Vapors and Gases). American Society for Testing and Materials.